Characteristic of eddies kinetic energy associated with yellowfin tuna in southern Java Indian Ocean

A Tussadiah[1*], W S Pranowo[1, 2], M L Syamsuddin[3], I Riyantini[3], B Nugraha[4], D Novianto[5]

[1] Marine and Coastal Data Laboratory, Marine Research Center, Agency of Research and Human Resources, Ministry of Marine Affairs & Fisheries Republic of Indonesia
[2] Department of Hydrography Engineering, Indonesian Naval Postgraduate School (STTAL)
[3] Padjadjaran University, Department of Marine Science, Fisheries and Marine Science Faculty, Padjadjaran University
[4] Fisheries Research Center, Ministry of Marine Affairs & Fisheries Republic of Indonesia
[5] Tuna Fisheries Research Institute, Ministry of Marine Affairs & Fisheries Republic of Indonesia
*e-mail: armyanda@gmail.com

Abstract. Eddies kinetic energy (EKE) is one of the most indicators in observed the phenomena of upwelling and down welling generated by circular current or eddies. This research aims are to determine the characteristics and intensity of eddies and EKE and its relation to the distribution of yellowfin tuna (*Thunnus albacares*) in Southern Java Indian Ocean. Based on Automated Eddies Detection (AED) method, it is succesfully discovered many eddies well formed in Southern Java Indian Ocean through 2014. Furthermore, EKE has a vary values to the depth, which tends to be higher at the surface layer than at thermocline layer. EKE in this region display a distinct seasonal cycle with maximum occurred in Southeast Monsoon and minimum in Northwest Monsoon. Increasing of EKE in Southeast Monsoon tend to be affected by currents system of Indonesian Throughflow (ITF) and South Equatorial Current (SEC). The highest of yellowfin tuna catches found in June 2014 and occurred in the current system with high EKE intensity. Correlation between eddies and yellowfin tuna found at thermocline layer (109 m) and occurred in cyclonic eddies ($R^2 = 0.59$).

1. Introduction

Indonesian archipelagos link the Pacific and Indian Oceans and play a crucial role in global ocean thermohaline circulation [1]. Furthermore, Tropical Indian Ocean interaction with the atmosphere plays an important role in shaping climate on either regional or global scales [2]. There are unique ocean currents that flow seasonally through Indian Ocean, among others are the Indonesian Throughflow (ITF) which links Pacific and Indian Ocean [3], the South Java Current (SJC) which flows along the south Java coast [4], and the South Equatorial Current (SEC) which flows westward from western Indian Ocean [5]. Despite this importance, many aspects of upper ocean dynamics are still unknown, especially of different types of motion and scales. Upper ocean variability is characterized by eddies, mostly geostrophic and generated by instabilities of ocean currents [6]. Eddies are important because it have so much kinetic energy, as well it is responsible for the irreversible mixing of waters with different properties. Eddies have a deep roots and can carrying energy and momentum to the seafloor [7].

Eddies are generally more energetic than the surrounding currents and are an important component of dynamical oceanography at all scales [8]. The fact that both cyclonic and anti-cyclonic eddies may embody either upwelling or downwelling in their centres [9]. *Note*: In Southern Hemisphere, "cyclonic eddies" rotate clockwise and "anti-cyclonic eddies" rotate counter clockwise (figure 2; red and black circles represent cyclonic and anticyclonic), vice versa in Northern Hemisphere. When cyclonic eddies occurred there may be nutrients in abundance, hence of the mixing water mass from bottom layer to the upper layer. This nutrient might be supports living organism through food chain start from plankton, small fish, up to pelagic fish, for instance tuna [4]. Tuna (*Thunnus.sp*) has a very high economic value in the world market. Hence, it is the most important fishery resources targeted by fisherman from various countries including Indonesia, also it is an important food source in the world [10].

In detection of eddies formation, a few method have been proposed, based either on the physical or geometrical characteristics of the flow field [11]. For instance by [12] using the higher resolution Sea Surface Height (SSH) fields afforded by the merged T/P and ERS-1 and ERS-2 satellite datasets, then by [13] using Sea Level Anomaly (SLA) maps from the multi satellite AVISO - product. Moreover, mesoscale eddies activities have been studied in the Eastern Indian Ocean associated with the South Equatorial Current (SEC). In Indian Ocean a high Eddies Kinetic Energy (EKE) intensity (around 150 to 250 cm^2/s^2) can be found around 25ºS extending westward from the Australian coast (figure 1) [14]. In Indian Ocean, there are several researches about eddies has been done. For instance by [14] about the formation and mechanism of eddy kinetic energy; by [15] about eddies variability and the oceanography characteristics at eddy centre; and by [16] which clearly clarify eddies mechanism in the South-eastern Tropical Indian Ocean.

Most of eddies studies in Indian Ocean are focused on the sea surface and little is known about the impact on the fisheries, specifically to tuna catches [17]. In this paper, we apply an oceanography data based on NEMO Model to study eddies structures and its association with tuna catches. In detection eddies formation, here we use the automatic eddies detection algorithm for the high-resolution numerical product developed by [11]. First of all, eddies data is set up by identifying cyclonic and anti-cyclonic eddies from the numerical product and then statistical analysis is applied. This paper is composed of five sections: Section 2 describes the physical oceanography model from NEMO Model through INDESO – KKP Project. Section 3 clearly identified eddies characteristics and intensity of EKE. Section 4 emphasizes a series of statistical analysis is applied to compute the coefficient correlation of eddies with tuna catches data from LPPT Benoa, Bali. Section 5 concludes the paper with summary.

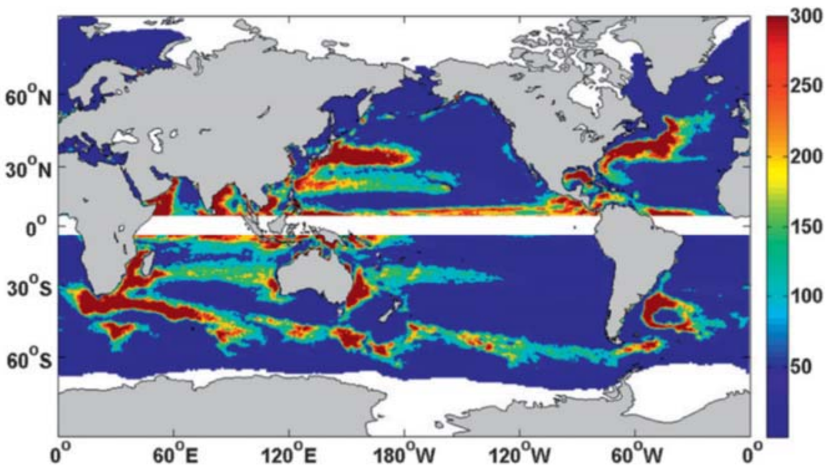

Figure 1. Global EKE (cm^2/s^2) calculated from the 15 years SLA [11].

2. Data

The data used in this study, including u and v components of sea current at two vertical level, which represents surface layer (mixed layer depth) at 5 m depth and thermocline layer at 109 m depth. This was generated by Nucleus for European Modeling of the Ocean (NEMO) Model through Physical Ocean Model of Infrastructure Development for Space Oceanography (INDESO) Project KKP [18]. INDESO-Project KKP is a collaboration project between Indonesia and France to improve the institutional capacity and human resources of oceanographic operational systems. Oceanographic data service has been running since 2014 through www.indeso.web.id [19].

NEMO model is a numerical simulation of the ocean. It have three components, which are: "blue-ocean" NEMO-OPA simulates the dynamics; the "white-ocean" NEMO-LIM simulates the sea-ice; and the "green-ocean" NEMO-TOP simulates the biogeochemistry [20]. The ocean physical model used for the INDESO projects is a regional configuration of the NEMO-OPA. These model is forced at the surface using 3-hourly ECMWF atmospheric analysis and forecast fields. [21].

The operational INDESO Physical Ocean Model system has a 1/12^o or 9.25 km x 9.25 km horizontal resolution and 50 vertical layers with increased resolution near the surface, also provides 10 days of 3D ocean forecast with updated weekly. This product includes daily mean fields of atmospheric fluxes, physical parameters (temperature, salinity, currents, sea level), hourly surface variables (SST, SSH, currents), as well as hourly values of all fields at selected mooring sites and validation metrics [18]. The NEMO 2.3 version was used in INDESO Project and has been developed at Mercator-Ocean. This regional ocean physical model provides physical fields for the past two weeks (forced by a global 2-weeks analysis) and ocean forecast (forced by a global 10-day forecast) for the next 10 days [21].

3. Seasonal Cycle of Eddies and EKE Variation

3.1. Eddy Variation and Characteristic

In detection of eddies occurrences was using the automatic eddy detection algorithm developed by [11]. This method can be applied to any velocity field and also has been validated by [11]. Basically the method was based on eddies characteristics, such as for the minimum velocities were indicates in the proximity of the eddy center, and the velocity values that increase gradually linear from its center up to reach the maximum near the edges. Furthermore, four constraints were defined on this method to identifying eddies occurrence based on the characteristics of eddy velocity fields, which: (i) along east-west section, meridional velocity (V) has to reverse in sign across the eddy center and its magnitude has to increase away from it; (ii) Along north-south section, zonal velocity (U) has to reverse in sign across the eddy center, and its magnitude has to increase away from it; (iii) the velocity magnitude has a local minimum at the eddy center; and (iv) around the eddy center, the directions of the velocity vectors have to change with a constant sense of rotation [22].

Based on automatic eddies detection it is found in Southern Java Indian Ocean mostly generated by cyclonic eddies rather than anticyclonic. In total of 474 cyclonic and 442 anticyclonic, found 192 cyclonic and 181 anticyclonic at the surface layer; as well at the thermocline found 282 cyclonic and 261 anticyclonic eddies. Generally cyclonic eddies mostly occurred during northwest season (at surface layer) and southeast season (at thermocline layer); meanwhile anticyclonic mostly occurred during first transition season (at surface layer) and second transition (at thermocline layer) [22]. From figure 2a there were two coloured circles, which are indicates red circle as a cyclonic eddy and black circle as an anticyclonic eddy. During northwest season (figure 2a), eddies dominantly generate in the Southern Indian Ocean along 16 – 20^{o}S, and there were several eddies occurred along the western Sumatera coast and reach to Southern Java. These eddies might be generated due to high shear velocity of SJC. As we can see in figure 2a, SJC flows eastward dominantly along the region with a strong velocity (red arrow) around 0.4 – 0.6 m/s. On the southeast season (figure 2b) the existence eddies near western Sumatera coast and southern Java decrease due to the weakness of SJC during this season. However, as seen in the figure 2b there were cyclonic eddies that existence in the southern coast Java during this season. This cyclonic eddies suggested was developed by the stronger ITF current system that flowing south-westward in this region [23]. Furthermore, from figure 2b showed that SEC current system flowing westward with a strong intensity (0.5 to 0.9 m/s). So thus, during southeast season eddies existences were moving southward to the offshore hence of the high intensity of SEC and ITF.

Eddies formation in the Southern Java Indian Ocean is not only generated by local wind but also by the remote forcing that generates SEC, ITF, and SJC [16]. The seasonally current flow in Southern Java Indian Ocean play an important role in eddies formation [24]. Thus, in the open ocean, mesoscale eddies that generate by the wind stress is not likely to be effective rather than by current flow pattern [9]. The mesoscale cyclonic eddies mostly appeared along the SJC current system near the southwest Sumatera coast to the southern Java, whereas the anticyclonic eddies mostly appear in the south of SEC current system. Occurrences of anticyclonic eddies also presumed generated by propagation of Rossby waves. Total eddies formation at two vertical layers predominantly rich at thermocline layer rather than surface layer. It is might be due to the high intensity of shear velocity at this depth, [23] stated that the eastward currents (SJC) form a large vertical shear in the depth range from 100 to 300 m in contrast with the westward current which is homogenized in the upper 300 m [24]. Furthermore, there were other factors in generating eddies vertically for instance local wind, topography, and propagation of Kelvin and Rossby waves.

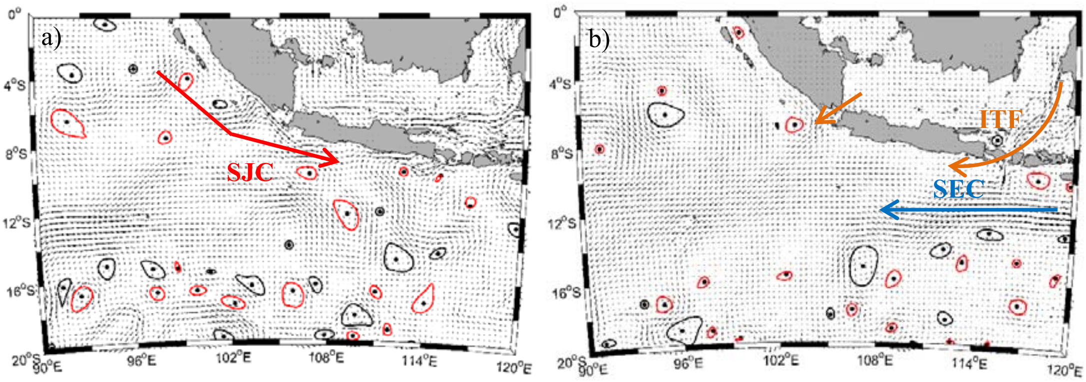

Figure 2. Eddies spatial distributions at surface layer in: a) Northwest Season and b) Southeast Season.

Histogram of eddies sizes at surface and thermocline layers are shown at figure 3. Both at surface and thermocline layers there are more cyclonic than anticyclonic eddies. The peak number at surface layer is located about 50 – 80 km, but for cyclonic eddies the frequencies may reach to 90 km. Whereas, at thermocline layer eddies sizes is greater than at surface layer, here the peak number is about 60 – 100 km. It has a similar results with what [25] found using surface satellite-tracked drifter data, which more sub-mesoscale eddies are densely over the entire Southern Indian Ocean (100 km > r > 60 km). Greater diameter at thermocline layer, presumed that eddies in this layer has a stronger intensity than at surface layer, which might be due to the high intensity of shear velocity at this depth as argued above.

The spatial distribution of eddies sizes is plotted at figure 4. Generally, eddies with larger diameter mostly found in the southern of Indian Ocean along 10° – 15°S. The spatial distribution of mesoscale cyclonic and anticyclonic eddies were different. As for the mesoscale anticyclonic eddies dominantly appears at the SEC pathways; whereas the mesoscale cyclonic eddies rich in the SJC pathways. It is consistent with [16] that mostly cyclonic eddies appears at the southern part of east Java coast; and for anticyclonic eddies at the south of SEC that flow westward, which are also as a part of Rossby waves. In the western Sumatera coast and southern Java, the shape of large eddies is restrained by difference in the velocity of SJC and the weaker currents around it as well as the morphology [16]. Furthermore, the submesoscale eddies generally occur below 15°S. It is consistent with [25] that medium eddies have a similar spatial distribution to that of large eddies but occur in a wider area. As well mention that the submesoscale eddies are densely distributed over the entire Indian Ocean, and for the appearance of submesoscale anticyclonic eddies might be due to the drifter aggregation maintained by converging Ekman currents.

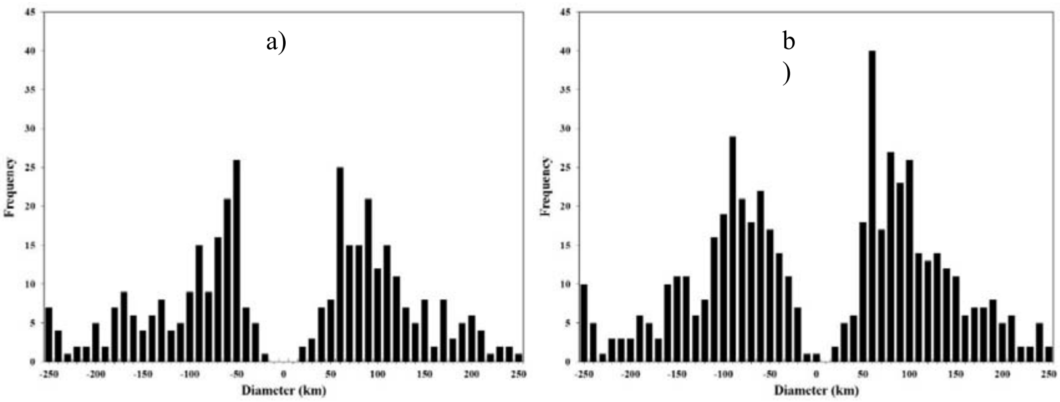

Figure 3. Histogram of eddies sizes at: a) surface layer; and b) thermocline layer; Positive (negative) eddy sizes represents cyclonic (anticyclonic) eddies.

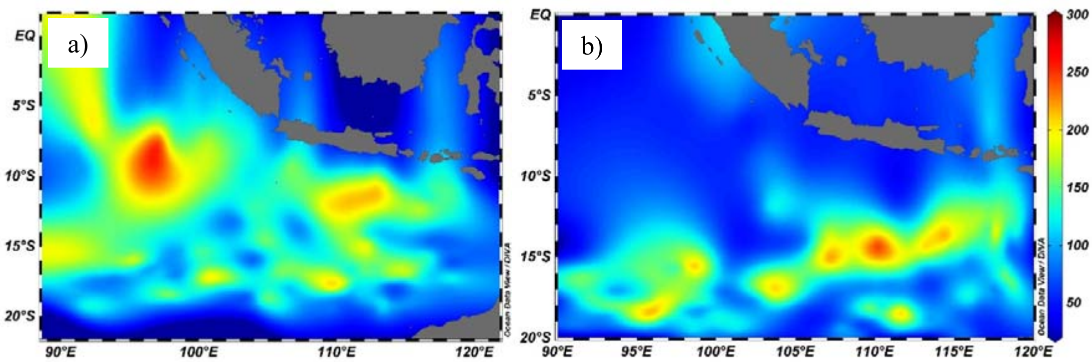

Figure 4. Eddies sizes distribution (km) at: a) cyclonic eddies; and b) anticyclonic eddies.

3.2. Seasonal Cycle of EKE Intensity

The EKE value is computed based on velocity components using the classical relation as follows:

$$\text{EKE} = \frac{1}{2}\left(U^2 + V^2\right) \qquad [8]$$

Where U and V are the zonal and meridional velocity components.

The EKE maps in the Southern Java Indian Ocean at four different seasons can be seen in figure 5. As shown in figure 5, EKE displays a distinct seasonal cycle with a maximum during southeast season (JJA) and 2nd transition season, and for a minimum during northwest season (DJF). The highest EKE (around 0.5 to 0.9 m^2/s^2) dominantly occurred along the ITF pathway near the Lombok Strait and in the south of SEC pathway along 12ºS. It is might be indicating moderate and intensive eddies activity over these regions. To further demonstrate the EKE seasonal cycle, we compute time series of EKE averaged and maximum value. Seasonal variations can be clearly identified, with a mean EKE of 0.03 m^2/s^2, a maximum of 1.52 m^2/s^2 in September; and a minimum around 0.02 m^2/s^2 in December. [14] suggested that the seasonal variations of EKE in the southeast Indian Ocean are predominantly regulated by baroclinic instability associated with the mean flows. Moreover, [14] states that there is phase about 2-4 months for the vertical shear precedes the EKE variation. This indicates that due to the peak ITF signal in April through July and the maximum occurs in early June [26], then the EKE values reach its maximum in September. As well the high EKE signal during September also generated by instability currents system of SEC. [27] state that SEC flows throughout the year and have a strong intensity in the southeast season along 10º – 20ºS [24]. This results also similar with [14] where the seasonal modulation of EKE in Southeast Indian Ocean is mediated by baroclinic instability associated with the underlying

IOP Conf. Series: Earth and Environmental Science **176** (2018) 012004 doi:10.1088/1755-1315/176/1/012004

westward-flowing SEC system and the surface eastward-flowing South Indian Ocean Countercurrent (SICC).

The mean EKE at cyclonic (anticyclonic) eddies centers could be calculated in the Southern Java Indian Ocean at surface layer giving average EKE 0.010 (0.012) m^2/s^2, and at thermocline layer giving average EKE 0.555 (0.313) m^2/s^2. From figure 6 can be seen the seasonal cycle of EKE at eddies centers. Generally, for both layers the cyclonic eddies have a larger EKE than anticyclonic. In the surface layer, EKE at cyclonic eddies reach its maximum on October, whereas the anticyclonic have a peak on November. However, in the thermocline layer larger EKE at cyclonic eddies found on June to October, while the anticyclonic on March and May. The high modulation of EKE at cyclonic eddies that occurred during southeast and 2nd transition season are mediated by geostrophic currents instability of SEC and ITF system. As argued above, that EKE modulation in this region is predominantly restrained by the instability mean flows of ITF and SEC. Furthermore, the results indicate that eddies in the thermocline layer has a higher intensity than in surface layer. As well the cyclonic eddies have a greater intensity in transporting water mass than anticyclonic. It is consistent with [28] that the energy of the downwelling generated by anticyclonic eddies tend to be weak.

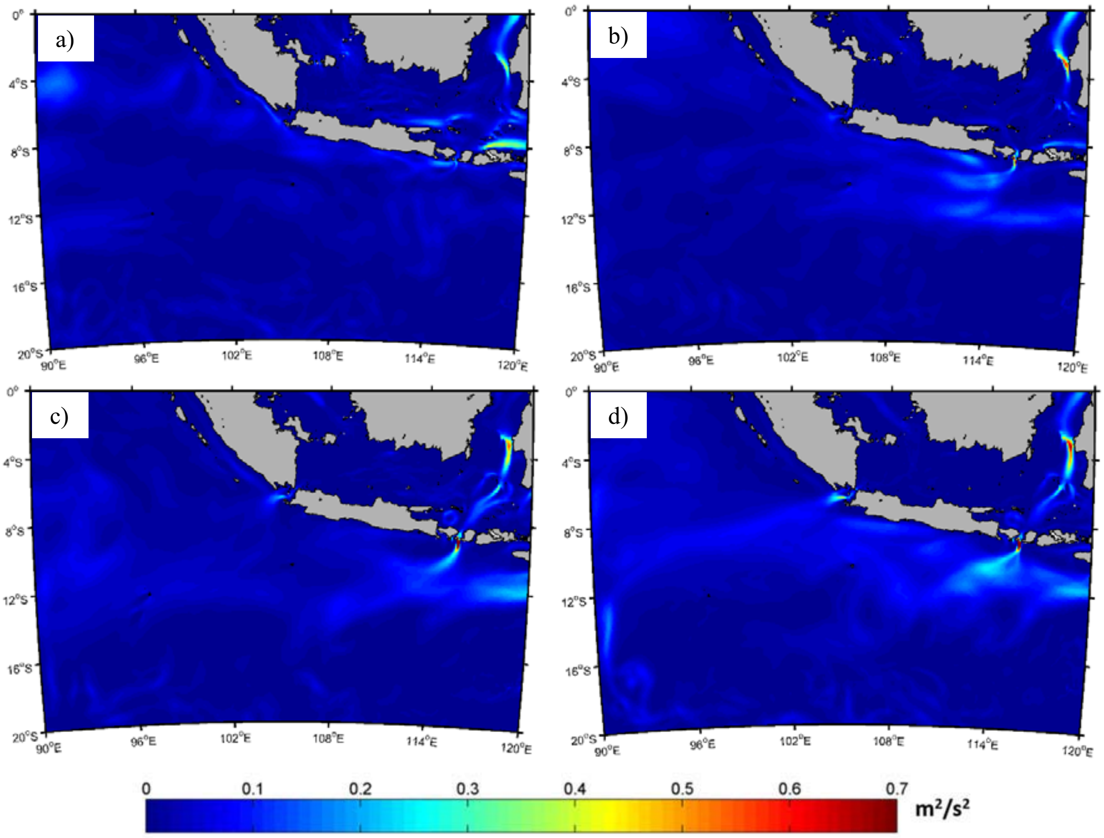

Figure 5. Seasonal distribution of EKE in: a) Northwest Season (Dec – Feb [DJF]); b) 1st Transition Season (Mar – May [MAM]); c) Southeast Season (Jun – Aug [JJA]); and d) 2nd Transition Season (Sep – Nov [SON]).

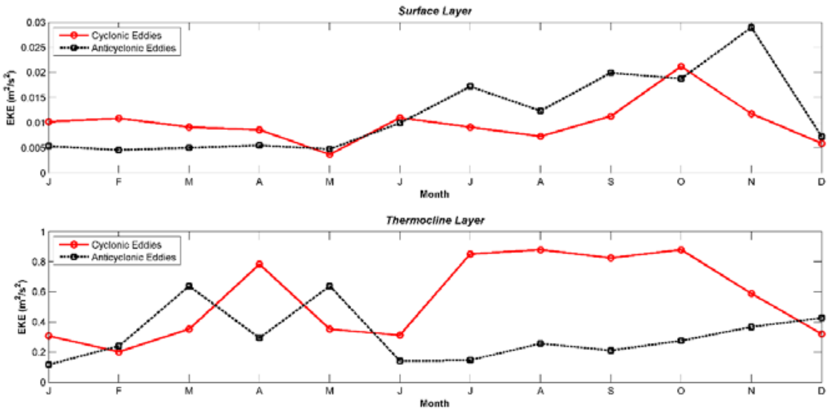

Figure 6. Mean seasonal of EKE at eddies centers.

4. Eddies and Yellowfin Tuna Catches

In analyse eddies and its association with the yellowfin tuna, we overlay eddies plot with the tuna catches, then used a statistical method which is Pearson's Correlation [22]. This correlation is to measure the strength of the association between two variables. Here we only compute the correlation for the thermocline layer, this refers to the yellowfin tuna catches data that predominantly appears in this layer [17]. The yellowfin tuna catches ware obtained from observation data by Loka Penelitian Perikanan Tuna (LPPT) Benoa in 2014 using a tuna longline. These tuna catches data represents as a frequency number of tuna caught in each month. The yellowfin tuna catches data can be seen on table 1.

Table 1. Yellowfin Tuna Catches on 2014.

Month	Yellowfin Tuna Catch
January	1
February	0
March	6
April	6
May	7
June	48
July	15
August	1
September	0
October	3
November	2
December	0

Based on the yellowfin tuna catches data, found the highest tuna catches was on June 2014; whereas the lowest on January 2014 [22]. Meanwhile, on February, September, and December no tuna catches were found. This is might be due because of the ships were not operated during these months. The overlay between eddies and tuna catches can be seen on figure 7 with the total of tuna caught represent as a yellow circle. On June 2014 (figure 7) yellowfin tuna catches found along in the edges either cyclonic or anticyclonic eddies. The yellowfin tuna distribution in this region probably due to the downwelling and upwelling generated by eddies. [9] mention that in the types of eddies where upwelling and divergence; downwelling and convergence often occur near the edges or in eddies outer edges. Thus, eddies motion in the ocean yield rich nutrients and further can support fisheries. Otherwise, yellowfin tuna catches not always found near in the edge of eddies. This indicates that there were other oceanographic parameters which are more influence on the abundance and distribution of yellowfin tuna, such as sea surface temperature, fronts, and depth of thermocline [29].

As the results of Pearson's Correlation found the highest correlation is in the cyclonic eddies (r = 0.59) rather than anticyclonic eddies (r = 0.14). A highest correlation between cyclonic eddies and yellowfin tuna might be due to the fishery abundance, hence the mixing water mass from bottom layer to upper layer [22]. Therefore, nutrients from bottom layer will be rising up and might be generated the primary productivity [17]. Furthermore eddies presumably localize tuna forage and then create a good feeding opportunity [30]. Moreover, the primary production increased within cyclonic rings in the Southern Hemisphere. The Coriolis effects force deflects water movement to the left away from the eddy center, and thus the depth of thermocline would be decreases and nutrients-rich waters closer to the surface layer and increasing primary production [31].

Based on the Pearson's correlation between EKE at eddies center and yellowfin tuna also found the highest correlation on the cyclonic eddies (r = 0.37). Strong correlation on EKE at cyclonic eddies is due to the larger EKE at this type rather than at anticyclonic eddies. This result also shows that EKE distribution has an influence in distribution of yellowfin tuna, besides the oceanographic parameters as mentioned above. Predominantly yellowfin tuna distributed in the area with the larger EKE. Moreover [32] state that high yellowfin tuna catches were most likely in locations where the surface ocean characteristics were: increased current shear (EKE), relatively shallow MLD [22], and increased of phytoplankton concentrations. [30] also found the association between EKE and other tuna species, where large catches of albacore were mostly concentrated in area with relatively high EKE and geostrophic velocities. This suggests that tunas are associated with eddies fields.

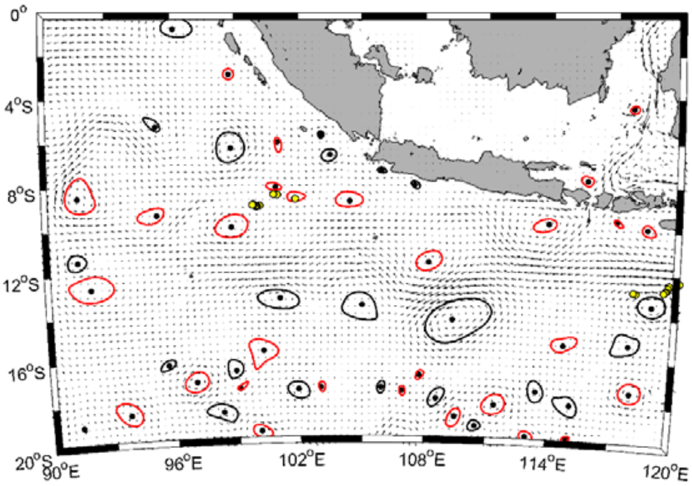

Figure 7. Eddies spatial distribution and yellowfin tuna catches.

5. Conclusion

Eddies appearances have been investigated by using the automatic eddies detection algorithm for the high resolution numerical product at two vertical layers in Southern Java Indian Ocean. In total of 916 eddies were detected, among 192 (181) are cyclonic (anticyclonic) eddies at the surface layer; as well at the thermocline 282 (261) are cyclonic (anticyclonic) eddies.

Predominantly for cyclonic eddies appear in the northwest season, whereas anticyclonic eddies appear in the 1st and 2nd transition season. These cyclonic and anticyclonic eddies appearances tend to followed the pattern of shear velocity current along in the Indian Ocean. As for the cyclonic eddies dominantly appear when a high intensity of SJC occurred. Meanwhile for the anticyclonic eddies suggest were associated with the appearance of SEC current system, as well with other forcing like Rossby wave. In addition, other local or nonlocal processes including local wind stress, kelvin waves, and topography may also modulate the activity of eddies in the Southern Java Indian Ocean.

Mesoscale cyclonic (anticyclonic) eddies populate along the SJC (SEC) system current, along 10^{o}S (15^{o}S). The spatial distribution of mesoscale eddies corresponds to the large EKE region. The EKE in this region shows a dis.tinct seasonal cycle with a maximum during southeast season (with maximum 1.52 m^2/s^2), and for a minimum during northwest season (with maximum 0.39 m^2/s^2). It is found that this seasonal modulation of EKE is mediated by the vertical velocity shear associated with the SEC and ITF currents system. Furthermore, by using the mean EKE as a background the mean EKE at eddies centers could be calculated. For cyclonic (anticyclonic) eddies at surface layer giving average EKE 0.010 (0.012) m^2/s^2, and at thermocline layer giving average EKE 0.555 (0.313) m^2/s^2. These results indicate that eddies in the thermocline layer has a higher intensity, as well the cyclonic eddies have a greater intensity in transporting water mass rather than anticyclonic eddies.

By overlying and using Pearson’s Correlation the association between eddies, EKE, and yellowfin tuna have been investigated. It is found that the yellowfin tuna catches not constantly found along eddies formation. Otherwise, the cyclonic eddies have a higher correlation ($r = 0.59$) with the yellowfin tuna rather than anticyclonic eddies. It is might be due to the nutrients in abundance in the cyclonic eddies, hence the mixing of water mass from bottom layer to the upper layer. As well for the EKE at cyclonic eddies center also has the highest correlation with yellowfin tuna ($r = 0.37$).

Acknowledgments
This work mostly conducted in the Marine and Coastal Data Laboratory (MCDL), Marine Research Center, Ministry of Marine Affairs & Fisheries Republic of Indonesia; and the Department of Marine Science, Padjadjaran University. The u and v sea surface current is provided by Physical Ocean Model at INDESO – Project KKP (http://www.indeso.web.id). The tuna catches data 2014 is provided by observers from Tuna Fisheries Institute, Benoa. Special thanks to the Fisheries Research Center and the Tuna Fisheries Research Institute, Ministry of Marine Affairs & Fisheries Republic of Indonesia; to Sharing Data Team from INDESO KKP; and also to KOMITMEN Research Group.

References
[1] Kartadikaria AR, Miyazawa Y, Nadaoka K and Watanabe A 2012 Existence of eddies at crossroad of the Indonesian Seas *Ocean Dyn.* **62** 31–44
[2] Schott FA, Xie SP and Jr. JPM 2009 Indian ocean circulation and climate variability *American Geo Union*. **47** 1–46
[3] Gordon AL, Sprintall J, Van Aken HM, Susanto D, Wijffels S, Molcard R, Ffield A, Pranowo Wm and Wirasantosa S 2010 The Indonesian throughflow during 2004-2006 as observed by the INSTANT program *Dyn Atmos Ocean*. **50** 115–28
[4] Pranowo WS, Phillips H and Wijffels S 2005 Upwelling event 2003 along south Java Sea and lesser Sunda Islands *J Segara*. **1** 119–26
[5] Bray NA, Wijffels SE, Chong JC, Fieux M, Hautala S, Meyers G and Morawits ML 1997 Characteristics of the Indo Pacific throughflow in the eastern Indian Ocean. **24** 2569–72
[6] Griffa A, Lumpkin R and Veneziani M 2008 Cyclonic and anticyclonic motion in the upper ocean *Geophys Res Lett.* **35**
[7] Tussadiah A, Syamsuddin ML, Pranowo WS, Purba NP and Riyantini I 2016 Eddy vertical structure in southern Java Indian Ocean : Identification using automated eddies detection. *Int J Sci Res.* **5** 967–71
[8] Chaigneau A, Gizolme A and Grados C 2008 Mesoscale eddies off Peru in altimeter records : Identification algorithms and eddy spatio-temporal patterns *Progress in Oceanography*. **79** 106–19
[9] Bakun A 2006 Fronts and eddies as key structures in the habitat of marine fish larvae : opportunity, adaptive response *Scientia Marina*. **70** 105–22
[10] Sukresno B, Hartoko A and Sulistyo B 2015 Empirical cumulative distribution function (ECDF) analysis of thunnus.sp using ARGO float sub-surface multilayer temperature data in Indian Ocean south of java *Procedia Environ Sci*. **23** 358–67 Available from: http://dx.doi.org/10.1016/j.proenv.2015.01.052
[11] Nencioli F, Dong C, Dickey T, Washburn L and Mcwilliams JC 2010 A vector geometry-based eddy detection algorithm and its application to a high-resolution numerical model product and high-frequency radar surface velocities in the Southern California Bight *J Atmos Ocean*

Technol. **27** 564–79
[12] Chelton DB, Schlax MG, Samelson RM and de Szoeke RA 2007 Global observations of large oceanic eddies *Geophys Res Lett.* **34** 1–5
[13] Chaigneau A, Texier M Le, Eldin G and Grados C 2011 Vertical structure of mesoscale eddies in the eastern South Pacific Ocean : A composite analysis from altimetry and Argo profiling floats *J Geophysical Research*. **116** 1–16
[14] Jia F, Wu L and Qiu B 2011 Seasonal modulation of eddy kinetic energy and its formation mechanism in the southeast Indian Ocean *J of Physical Oceanography*. **41** 657–65
[15] Pranowo WS, Tussadiah A, Syamsuddin ML, Purba NP and Riyantini I 2016 Karakteristik dan variabilitas eddy di Samudera Hindia selatan jawa *J Segara*. **12** 159–65
[16] Hanifah F, Ningsih NS and Sofian I 2016 Dynamics of eddies in the southeastern tropical Indian Ocean *J Phys Conf Ser*. **739** 12042
[17] Pranowo WS, Kuswardani ARTD, Nugraha B, Novianto D, Muawanah U, Prihatno H and Yu W 2016 Ocean-climate interaction of south eastern Indian Ocean for tuna fisheries & its socio-economy impacts *Int J Sci Res.* **5** 1956–61
[18] Purba NP and Pranowo WS 2015 *Dinamika oseanografi, deskripsi karakteristik massa air dan sirkulasi air laut* UNPAD Press Bandung ISBN : 978-602-0810-20-1 276 p
[19] Tussadiah A, Subandriyo J, Novita S and Pranowo WS 2017 Verification of PISCES dissolved oxygen model using in situ measurement in Biak, Rote, and Tanimbar Seas, Indonesia *Int J Remote Sens Earth Sci*. **14** 37–46
[20] Levy C and Benshila R 2012 NEMO for Dummies *Mercat Ocean Q Newslatter*. **2** 4–7
[21] INDESO - KKP 2015 Product user manual – physical model outputs 1–17
[22] Teliandi D, Djunaedi OS, Purba NP and Setiyo W 2013 Relationship between variability mixed layer depth $\Delta T=0.5\ ^{o}C$ criterion and distribution of tuna in the eastern Indian Ocean **2** 162–71
[23] Syamsudin F and Kaneko A 2013 Ocean variability along the southern coast of Java and Lesser Sunda Islands *J Oceanogr*. **69** 557–70
[24] Mustikasari E, Dewi LC, Heriati A and Pranowo WS 2015 Pemodelan pola arus barotropik musiman 3 dimensi (3D) untuk mensimulasikan fenomena upwelling di Perairan Indonesia *J Segara.* **11** 25–35
[25] Zheng S, Du Y, Li J and Cheng X 2015 Eddy characteristics in the South Indian Ocean as inferred from surface drifters *Ocean Sci*. **11** 361–71 Available from: http://www.ocean-sci.net/11/361/2015/
[26] Potemra JT 1999 Seasonal variations of upper ocean transport from the Pacific to the Indian Ocean via Indonesian Straits *J Phys Oceanogr*. **29** 2930–44
[27] Utamy RM, Purba NP, Pranowo WS and Suherman H 2015 The pattern of south equatorial current and primary productivity in south Java Seas *Int Proc Chem Biol Environ Eng*. **51** 139–42
[28] Oki D and Putri MR 2014 Identifikasi awal eddies di perairan Laut Jawa **1** 12-20
[29] Rajapaksha JK, Nishida T and Samarakoon L 2010 Environmental preferences of yellowfin tuna (*Thunnus albacores*) in the northeast Indian Ocean : an application of remote sensing data to longline catches 1-6
[30] Zainuddin M, Kiyofuji H, Saitoh K and Saitoh SI 2006 Using multi-sensor satellite remote sensing and catch data to detect ocean hot spots for albacore (*Thunnus alalunga*) in the northwestern North Pacific *Deep Res Part II Top Stud Oceanogr*. **53** 419–31
[31] Abigail W, Zainuri M, Tisiana A, Kuswardani D and Setiyo W 2015 Distribution of nutrient, light intensity, chlorophyll-a and water quality in Badung Strait, Bali during southeast monsoon *Depik*. **4** 87–94
[32] Dell J 2012 Fisheries oceanography of yellowfin tuna (*Thunnus albacares*) in the Tasman Sea *Tasmania Univ.*